BIOORGANIC CHEMISTRY 18, 63–77 (1990)

The Hydrolysis of a Co(III) Chelated Amide Catalyzed by an Internal Phosphonic Acid Group

JAMES LIGHT AND RONALD BRESLOW[1]

Department of Chemistry, Columbia University, New York, New York 10027

Received June 21, 1989

In a previous study it was found that an internal carboxylate ion contributed nothing to the rate of hydrolysis of a Co(III) complex of a glycine anilide, although in the enzyme carboxypeptidase A the catalyzed hydrolysis of peptides is performed by a carboxylate and a Zn^{2+} ion. However, external acetate ion and even more so external phosphate ion were effective cocatalysts. In the current work we have incorporated a phosphonate ion as an internal cocatalyst for the hydrolysis of a Co(III) complex of a glycine anilide, in two different versions. The internal phosphonate group indeed proves to be effective. The contrast with an ineffective carboxylate ion may in part reflect a different stereoelectronic requirement, but a principal contributor is the increased basicity of the phosphonate group. Its pK_a is still not as high as that of the abnormal carboxylate in the enzyme. It is suggested that phosphate or phosphonate groups may be better models than carboxylate ions for the abnormally basic carboxylates found in some enzymes.

INTRODUCTION

The enzyme carboxypeptidase A catalyzes the hydrolysis of peptides, and related artificial substrates, using a Zn^{2+} and the CO_2- group of Glu-270 as the principal catalytic functionalities (*1, 2*). Although several possible mechanisms have been proposed (*2–4*), we favor a process (Scheme 1) in which the Zn^{2+} coordinates to the amide carbonyl and the carboxylate performs several proton transfers (*5, 6*). A key feature of our proposal is that the carboxylate not only delivers a hydroxide ion in step 1, acting as a general base, but it also does a double proton transfer in step 2. This proposal was based on our finding (*5, 6*) that in a model system such amide cleavage is best performed by buffer species such as acetate and phosphate that can use a two-proton transfer mechanism. It also best explains our earlier finding (*7*) that carboxypeptidase cannot use methanol instead of water in its reactions, since in the mechanism of Scheme 1 *both* protons of water are required.

We have described a study of a Co(III) amide complex, compound **1** (Scheme 2), and some derivatives such as **2** and **3** (*5*). A related study has also been reported (*8*). We found that an internal carboxylate group, as in **2** and **3**, added nothing to the rate of hydrolysis of the amide group. Indeed, the phenolic group of

[1] To whom correspondence should be addressed.

0045-2068/90 $3.00

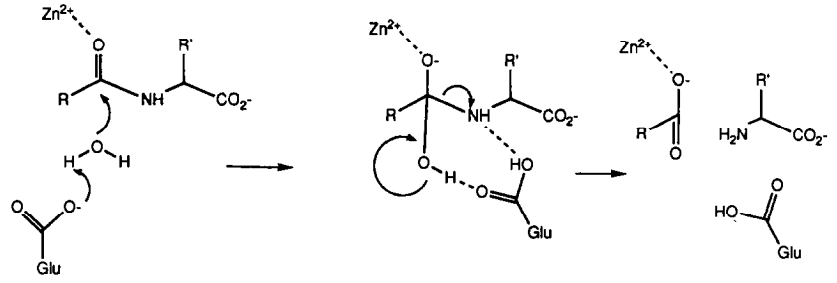

SCHEME 1. Our proposed two-proton transfer mechanism for catalyzed peptide hydrolysis by carboxypeptidase A.

3 was more effective as a catalyst if the carboxylate group was missing. Of course, in the enzyme itself the phenolic group of tyrosine 248 is now known not to play a catalytic role (*9*). Interestingly, an *external* carboxylate group was catalytic—acetate buffer assisted the cleavage of **1** (*5*).

We ascribed the difference to two factors: (i) acetate ion is more basic than is the internal carboxylate of **2** or **3**, which have abnormally low pK_a's near 2.0 because of proximity to the Co(III) and (ii) the stereoelectronic preference (*10*) for proton abstraction by a carboxylate ion can be satisfied by an external carboxylate ion but not by the internal carboxylate groups of **2** or **3**. Thus the pK_a for internal proton abstraction by the carboxylates in **2** or **3** will be even lower than their titration pK's.

Consistent with the basicity argument, the more basic phosphate buffer was even more effective in assisting the cleavage of **1** than was acetate buffer. In fact, phosphate was so effective that it reached kinetic saturation at quite low concentrations. Thus an obvious question arose: would an internal phosphate group be an effective catalyst in structures related to **2** or **3**, in place of the noncatalytic carboxylate group? Its higher pK_a should make it more like the carboxylate ion of Glu-270 in the enzyme, which has (*11*) the abnormally high pK_a of 6.1. Furthermore, the stereoelectronic effects in phosphates (*12*) are not as well established as in carboxylates, and they are probably smaller.

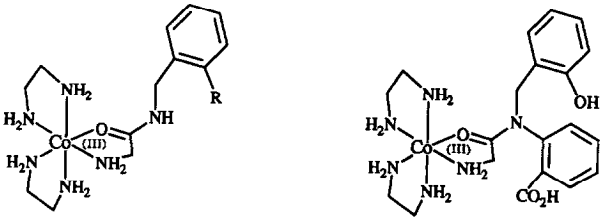

1 R=H
2 R=CO_2H

3

SCHEME 2. Some compounds whose hydrolyses were examined in our previous study.

We concluded that an internal phosphonate group was more attractive than a phosphate, for stability reasons. As we describe later, methylphosphonate buffer is even more effective than is phosphate buffer as an external catalyst. Thus we have synthesized the phosphonate complex **4**, and the related compound **5**. As hoped, the internal phosphonate groups of **4** and **5** indeed proved to be catalytic in cleaving the amide links. Furthermore, in **4** this internal catalysis replaces the external catalysis by buffers, showing that it operates in the same steps. However, even this more effective internal catalysis does not bring the cleavage rate up to that for the enzymatic processes it mimics.

MATERIALS AND METHODS

Substrates

All compounds are characterized by proton NMR and ir spectroscopy. The following abbreviations are used in the description of NMR spectra: s = singlet, d = doublet, t = triplet, m = multiplet (not first order), bs = broad singlet (line width approximately 1 Hz or greater), etc. The coupling constants given are the apparent coupling constants measured from the centers of the peaks.

The preparation of **4** is shown in Scheme 3. Diethyl 2-aminophenylphosphonate **10** was synthesized by the method of Bulot *et al.* (*13*). Compound **10** was coupled

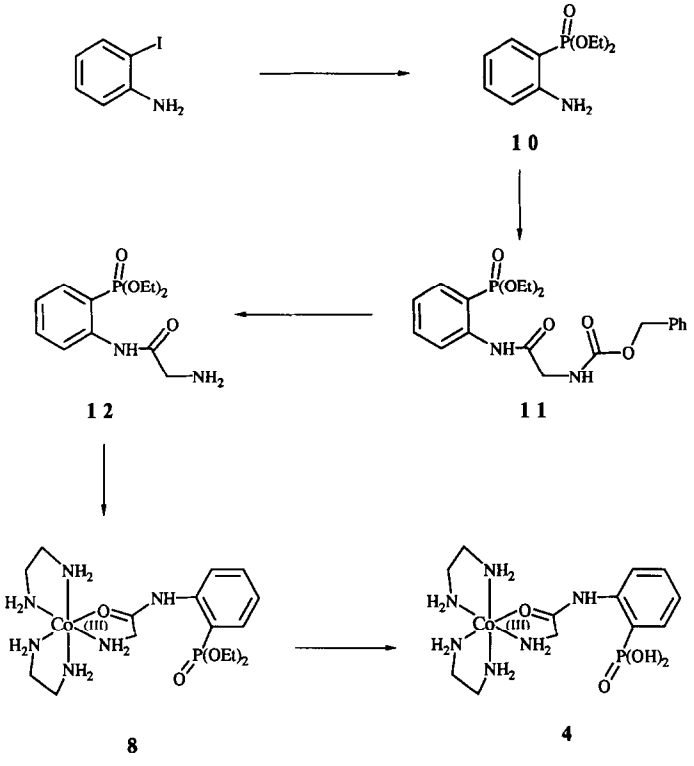

SCHEME 3. The synthetic route to **4**. The other cobalt complexes were synthesized by similar routes.

with *N*-carbobenzyloxyglycine using *N*-ethyl-*N'*-(3-dimethylaminopropyl)carbodiimide in the normal way, to afford the amide **11** in 52% yield, mp 100–101°C. Catalytic hydrogenation of **11** using 10% Pd/C in ethanol gave a 99% yield of glycine derivative **12**. The following ^{1}H NMR spectra were obtained: **10** ($CDCl_3$, 200 MHz) δ 7.42 (d of d of d, 1H, $^3J_{H\text{-}P}$ = 14.3, J_{ortho} = 7.7, J_{para} = 1.6 Hz), 7.25 and 7.21 (d of t under $CHCl_3$, 1H), 6.67–6.59 (m, 2H), 5.14 (bs, 2H), 4.2–4.0 (m, 4H), 1.31 (t, 6H); **11** ($CDCl_3$, 200 MHz) δ 10.94 (bs, 1H), 8.62–8.52 (3 peaks with shoulders, 1H), 7.62–7.50 (m, 2H), 7.40–7.3 (m, 5H under $CHCl_3$), 7.16 (t of d, 1H), 5.50 (bs, 2H), 5.17 (s, 2H), 4.2–4.4 (m, 4H), 1.29 (m, 6H); **12** (d_6-DMSO, 300 MHz) δ 8.42 (d of d, 1H, *J* = 7, 0.9 Hz), 7.68 (d of d of d, 1H, $^3J_{H\text{-}P}$ = 14.6 Hz, *J* = 7.7, 1.5 Hz), 7.59 (apparent t of t, 1H, *J* = 7.4, 1.2 Hz), 7.29 (apparent t of d of d, 1H, *J* = 7.5, 3.2, 1.1 Hz), 4.05 (m, 4H), 3.28 (s, 2H), 1.23 (t, 6H). The CI MS of **11** showed M + 1 at 421. The CI MS of **12** showed M + 1 at 287.

Compound **12** was converted to the $(en)_2Co(III)$ complex **8** by a procedure analogous to that we have described earlier (*5*) for other glycine derivatives. Stirring **12** with 1 eq $(en)_2CoBr_2 \cdot Br$ in ethanol coordinated the amino group, and then $AgNO_3$ coordinated the amide carbonyl. The complex **8** was isolated by ion-exchange chromatography (SP-C25) in 52% yield. ^{1}H NMR of **8** was (d_6-DMSO, 300 MHz) δ 12.03 (s, 1H), 7.8–7.7 (m, 3H), 7.5 (bt, 1H), 6.6 (bd, 1H), 6.4 (bs, 2H), 6.1 (bs, 2H), 5.8 (bd, 2H), 5.6 (bs, 1H), 5.5 bs (1H), 4.9 (bs, 1H), 4.2–4.0 (bm, 4H), 4.0–3.4 (bm, 2H), 2.7 + 2.5 + 2.3 (each a bs under DMSO, 8H), 1.30 and 1.25 (overlapping t, 6H). The free phosphonic acid derivative **4** was then prepared by heating 0.38 g **8** with 3.3 ml trimethylsilyl bromide in 11 ml dimethylformamide for 2 days at 40–45°C. Ion-exchange chromatography (SP-C25) afforded **4** in 91% yield. ^{1}H NMR of **4** (d_6-DMSO, 300 MHz) δ 7.8 + 7.74 + 7.69 (bt, bd, bd, 2H), 7.57 (bt, 1H), 7.40 (bt, 1H), 6.4–6.2 (bs, 2H), 6.15–6.11 (bs, 2H), 5.92–5.81 (bs, 2H), 5.82 (bs, 1H), 5.58 (bs, 1H), 4.89 (bs, 1H), 4.12 (bs, 1H), 4.60–3.2 (hump, 2H), 2.72 + 2.56 + 2.57 (3 bs under DMSO, 10H). The elemental analysis for **4** was as follows: Found (Calcd for $C_{12}H_{27}CoN_6O_4P \cdot Cl_3$) C, 27.06 (27.96); H, 5.32 (5.28); N, 15.54 (16.29); P, 5.77 (6.01); Co, 10.46 (11.43). We were not able to obtain a satisfactory elemental analysis for any of the complexes because of contamination from the Sephadex ion-exchange resin used to purify the complexes as described later. Dowex resins were found to be ineffective and all attempts to crystallize the complexes failed. However, we believe that the complexes are sufficiently pure for the following reasons: (i) the NMR spectra show no extraneous peaks, (ii) the ir and uv data agree with the spectra obtained for a compound whose crystal structure was previously determined (*5*), (iii) expected substrate hydrolysis products were measured by HPLC, and (iv) a catalytic impurity that might affect the rate is not present since changing the initial substrate concentration did not affect the measured pseudo-first-order rate constant.

Compound **5** was prepared in a similar fashion (Scheme 4). Starting with known (*14*) 2-aminophenylmethylphosphonic acid diester **13**, compound **15** (*N*-(*N'*-carbobenzyloxyglycyl)-2-aminophenyl)methylphosphonic acid diethyl ester was synthesized in 93% yield. Deprotection of **15** gave **16** (*N*-glycyl-2-aminophenyl) methylphosphonic acid diethyl ester in 98% yield. Compound **16** was coupled to *trans*-$(en)_2CoBr_2Br$ (37% yield) and then deprotected (97% yield) to give **5**. The ^{1}H

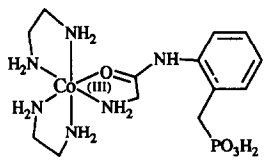

5

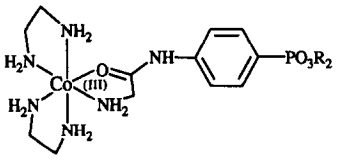

6 R=H
9 R=Et

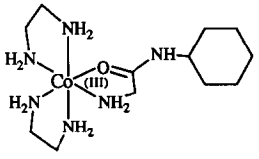

7

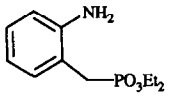

13

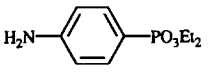

14

SCHEME 4. Other models and intermediates used in this study.

NMR of these compounds follow **13** ($CDCl_3$, 200 MHz) δ 7.11–7.00 (m, 2H), 6.74 (t, 2H), 4.28 (hump, 1.5H), 4.10–3.90 (m, 4H), 3.11 (d, 2H, $^2J_{H\text{-}P}$ = 21.9 Hz), 1.23 (t, 6H); **15** ($CDCl_3$, 200 MHz) δ 9.80 (bs, 1H, exchanges with D_2O), 7.75 (d, 2H), 7.35–7.29 and 7.12 (multiplets, 7H), 5.60 (bs, 1H, exchanges with D_2O), 5.15 (s, 2H), 4.08 (d, 2H, s with D_2O), 4.06–3.90 (m, 4H), 3.12 (d, 2H, $^2J_{H\text{-}P}$ = 21 Hz), 1.20 (t, 6H); **16** (CD_3OD, 300 MHz) δ 7.43 (d, 1H, J = 8.1 Hz), 7.14–7.04 (m, 2H), 7.00 (t, 1H, J = 7.5 Hz), 3.89–3.83 (m, 4H), 3.29 (s, 2H), 3.12 (d, 2H, $^2J_{H\text{-}P}$ = 21.3 Hz), 1.06 (t, 6H); **5** (d_6-DMSO, 300 MHz) δ 12.02 (s, 1H), 7.42–7.40 (m, 1H), 7.28–7.2 (m, 3H), 6.21 + 6.13 + 6.01 (each bs, 5H), 5.77 (bs, 2H), 5.32 (bs, 2H), 4.84 (bs, 1H), 4.12–4.4 (m, 2H), 3.23 (d of d, 1H, $^2J_{H\text{-}P}$ = 21.5 Hz, $^1J_{H\text{-}H}$ = 14.6 Hz), 3.05 (d of d, 1H, $^2J_{H\text{-}P}$ = 21.5 Hz, $^1J_{H\text{-}H}$ = 14.6 Hz), 2.75–2.4 (bm, 10H under DMSO), 2.4–2.2 (bs, 2H). The analysis of **5** was performed and again (vide supra) showed some impurities: (Calcd. for $C_{13}H_{29}CoN_6O_4P \cdot Cl_3$) C, 27.83 (29.48); H, 5.52 (5.46); N, 15.53 (15.86).

In a similar manner the known (*15*) diethyl ester of 4-aminophenylphosphonic acid **14** was converted to the cobalt complex **6** via the diester **9** with yields similar to the *ortho* series. The ^{1}H NMR spectra were as follows: **14** ($CDCl_3$, 200 MHz) δ 7.56 (d of d, 2H, J = 8.6, $^3J_{H\text{-}P}$ = 12.8 Hz), 6.67 (d of d, 2H, $^4J_{H\text{-}P}$ = 3.6, J = 8.6 Hz), 4.04 (m, 6H), 1.20 (t, 6H); *N*-(*N'*-carbobenzyloxyglycyl)-4-aminophenylphosphonic acid diethyl ester ($CDCl_3$, 200 MHz) δ 8.9 (bs, 1H), 7.8–7.6 (m, 4H), 7.35 (s, 5H), 5.8 (bt, 1H), 5.14 (s, 1H), 4.1–4.0 (m, 6H), 1.29 (t, 6H); *N*-glycyl-4-aminophenylphosphonic acid diethyl ester ($CDCl_3$, 200 MHz) δ 9.64 (bs, 1H), 7.82–7.69 (m, 4H), 4.15–4.02 (m, 4H), 3.48 (s, 2H), 1.30 (t, 6H); **9** (d_6-DMSO, 300

MHz) δ 12.70 (bs, 1H), 7.82–7.66 (m, 4H), 6.27 (bs, 3H), 5.98 (bs, 2H), 5.84 (bs, 1H), 5.4 (bs, 2H), 4.9 (bs, 1H), 4.14 (bs, 1H), 4.0 (m, 4H), 2.78–2.39 (humps, 10H under DMSO), 1.21 (t, 3H), 1.15 (t, 3H); **6** (d_6-DMSO, 300 MHz) δ 12.55 (s, 1H), 7.70–7.62 (m, 4H), 6.4–5.8 (5 broad humps, 7H), 5.4 (bs, 2H), 4.9 (bs, 1H), 4.1 (bs, 2H), 2.8–2.4 (4 humps under DMSO, 10H).

The simple cyclohexyl derivative **7** was prepared from *N*-glycylcyclohexylamine. ^{1}H NMR of **7** (d_6-DMSO, 300 MHZ) δ 10.0 (d, 1H), 6.3–5.6 (4 peaks, 6H), 5.6–5.2 (3 peaks, 3H), 4.8 (bs, 1H), 3.9 (bs, 2H), 3.5 (peak under H_2O), 2.3–1.9 (4 b peaks under DMSO, 8H), 1.8–1.5 (3 peaks, 6H), 1.2 (bd, 4H).

Other Materials

Water was distilled and deionized. The following amino sulfonate buffers were obtained from Sigma: 2-(*N*-morpholino)ethanesulfonic acid, Mes, pK_a 6.1; *N*-2-hydroxyethylpiperazine-*N'*-2-ethanesulfonic acid, Hepes, pK_a 7.5; *N*-(2-hydroxyethyl)-piperazine-*N'*-3-propanesulfonic acid, Epps, pK_a 8.0; 2-(*N*-cyclohexylamino)ethanesulfonic acid, Ches, pK_a 9.3; and 3-(cyclohexylamino)propanesulfonic acid, Caps, pK_a 10.4. All amino sulfonate buffers were recrystallized from ethanol/water and dried *in vacuo* over P_2O_5. *trans*-Dibromobis(ethylenediammine)cobalt(1+) bromide, $(en)_2CoBr_2 \cdot Br$, was made by the method of Jackson *et al.* (*16*). Bis(ethylenediammine)glycinatocobalt(2+) dichloride was prepared from *trans*-$(en)_2CoCl_2 \cdot Cl$ by the method of Harrison and Nolan (*17*).

Buffers were freshly prepared and used within 3 days. Ionic strengths were maintained at I = 1.0 M, treating all activity coefficients as unity. Phosphate buffer was prepared from KH_2PO_4, by adjusting the pH to 7.20 with KOH solution and then diluting to volume. Methylphosphonate buffer was prepared from recrystallized, dried methylphosphonic acid and adjusted to pH 7.20 with KOH_{aq}.

TLC plates were kieselgel 60 F_{254} from EM Science. Flash silica gel was from ICN Biomedicals, 32-63, 60 Å pore size. Sephadex SP-C25 ion-exchange resin from Sigma was swollen in 0.1 M HCl for 12 h and washed with water until eluant had a neutral pH.

Kinetics

uv method. For uv kinetics and uv–vis spectra a Beckman DU-8 or DU-8B interfaced with a MacIntosh computer were used. For each complex, a stock solution of 6.3 to 8.4 mg of complex in 1.00 ml water was made (for the ester complexes, 1 drop 0.1 M HCl was added before dilution). The rates of hydrolysis did not vary with a threefold increase in complex concentration. Each stock solution was divided into 50-μl aliquots into glass ampules, which were sealed and stored frozen.

For each experiment, 1.00 ml of buffer in a semi-micro-quartz cuvette was equilibrated to 45.0 ± 0.1°C for at least 30 min in the thermostatted cell holder of the spectrophotometer. Then 5.0 to 8.0 μl of stock solution (to give A_0 = 1.0 ± 0.2) was added to each cuvette, the samples were mixed, and the absorbance change was measured at time intervals. The complex concentration was between 5 and 8 × 10^{-5} M. Generally, at least 40 data points for each experiment were

recorded, and the reactions followed for more than 5 half-lives. Some of the slower reactions ($t_{1/2} \approx 1$ day) were only followed for ≈3 half-lives. Absorbance changes were between 0.2 AU for the ester complexes and 1.0 AU for the acid complexes, depending on pH. The data were analyzed as a pseudo-first-order reaction, using the KORE program by Swain (*18*). All correlation coefficients were >0.9999, and the calculated standard deviations <1%.

For the pH rate profiles, the following buffers (pH range) were used: Mes (5.9–6.9), Hepes (7.0–7.6), Epps (8.0–8.5), Ches (9.5), and Caps (10.5). For each pH, the rate of hydrolysis was measured at five different buffer concentrations, 0.025 to 0.25 M. The rate was extrapolated to [buffer] = 0 by a linear least-squares line fit. The intercepts, the buffer uncatalyzed rate constants, are reported.

The effects of phosphate and methylphosphonate buffer concentrations were measured at pH 7.20 in the presence of 0.025 M Hepes to maintain pH. Corrections for catalysis by this added Hepes buffer are smaller than the experimental error.

Every experiment was duplicated at least once with freshly prepared buffer. All rate constants are the average of two or more independent kinetic runs. The confidence limits are reported at the 95% level.

HPLC method. The hydrolysis of cyclohexyl model **7** was studied by preparing 2.5 mM solutions of **7** in 5.0 ml of the buffers listed in Table 3. Each experiment was duplicated. These solutions were placed in test tubes, sealed with a septum, and placed in a 45 ± 1°C water bath for 42 days. At time intervals, 100-μl aliquots were withdrawn, quenched in 1.00 ml of 1 mM HCl, sealed, and frozen for simultaneous analysis at a later time. The amount of $(en)_2CoGlyO^{2+}$ produced at different times was measured by ion pair HPLC. The rate constants were calculated from linear least-squares analysis of ln(area of $(en)_2CoGlyO^{2+}$) vs time. The HPLC instrument consisted of two Waters 501 pumps controlled by an automatic gradient controller and a Waters 481 Lamba Max LC spectrophotometer. A 10-μl sample loop in a Rheodyne 7125 injector and an IBM ODS (C-18 reverse phase) column were also used. The chromatograms were recorded on a Spectra Physics 4270 electronic integrator.

The eluant for the ion pair HPLC was 55% methanol (Fisher HPLC, filtered) to 45% water solution (filtered). The water solution was made by dissolving 20.8 g sodium hexanesulfonate (Aldrich) and 2.3 g polyphosphoric acid (Aldrich) in 1000 ml distilled deionized water. Typical retention times with a flow rate of 0.8 ml/min were 3 min for the solvent front, 5 min for $(en)_2Co(glyO)^{2+}$, and 16 min for $(en)_2Co(glyNHC_6H_{11})^{3+}$.

RESULTS AND DISCUSSION

The amide groups of compounds **4–9** are hydrolyzed to give the glycinato cobalt species and the free aniline or amine. For example, cyclohexyl model **7** gives $(en)_2CoglyO^{2+}$ and cyclohexylammonium ion at the pH's studied. All hydrolyses were studied at 45°C, with ionic strength maintained at 1.0 M using KCl. All solutions were buffered with the appropriate amino sulfonate buffers listed under Materials

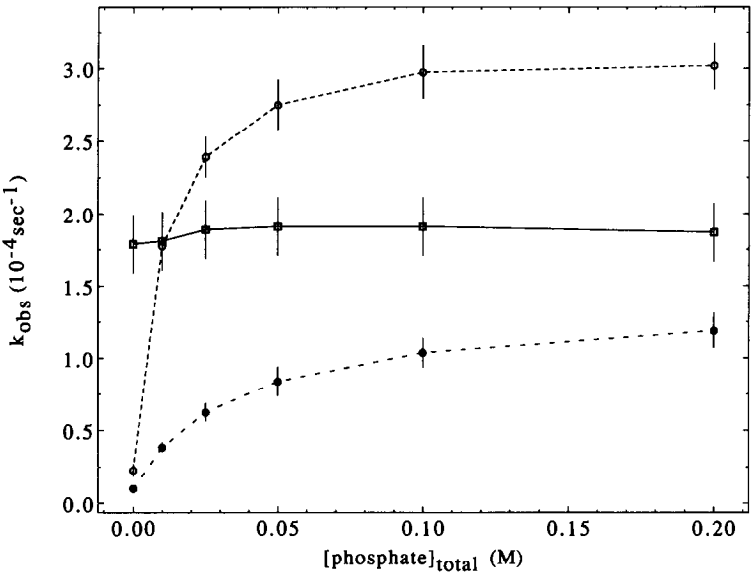

FIG. 1. The effects of phosphate buffer on the rates of hydrolysis of **4** (□), **5** (●), and **6** (○). The lines are simple interpolations. The error bars represent 95% confidence limits, calculated from the SD of two or more measurements. T = 45°C, I = 1.0 **M**, pH 7.20.

and Methods. These buffers are known not to chelate metal ions. Pseudo-first-order rate constants for compounds **4, 5, 6, 8,** and **9** were measured by computer analysis of the uv absorbance change vs time. The much slower hydrolysis of **7** was studied by using ion pair HPLC to measure the amount of $(en)_2CoglyO^{2+}$ produced at successive time intervals. Evidence that the uv change is due to amide hydrolysis has been presented in the earlier paper (*5*) and was confirmed here for **6** in the presence of 0.2 M phosphate. The same pseudo-first-order rate constant (within 3%) of 3.0×10^{-4} s^{-1} is obtained using either the HPLC peak area of $(en)_2CoglyO^{2+}$ or the uv absorbance change for the same samples.

One might expect the rate of hydrolysis of a compound with an efficient intramolecular catalyst to be independent of an external buffer catalyst. Therefore, the pseudo-first-order rates of hydrolysis of the models were measured at different total concentrations of phosphate buffer. The results are summarized in Figs. 1 and 2.

The hydrolysis rate of the *ortho*-phosphonic acid **4** is indeed unaffected by phosphate buffer, but those of the *ortho*-methylenephosphonic acid **5** and of the *para*-phosphonic acid **6** increase with increasing phosphate buffer concentration to plateaus at [phosphate]$_{total}$ > 0.2 M. Further increases in [phosphate]$_{total}$ up to 2.5 M give no further increase. When no phosphate buffer is present, the *ortho*-phosphonic acid **4** hydrolyzes nine times faster than *para* acid **6**. This ninefold increase suggests that the *ortho*-phosphonic acid group catalyzes the amide hydrolysis. The catalytic rate increase may actually be greater, considering that *ortho* substituted anilides usually hydrolyze more slowly than their *para* isomers

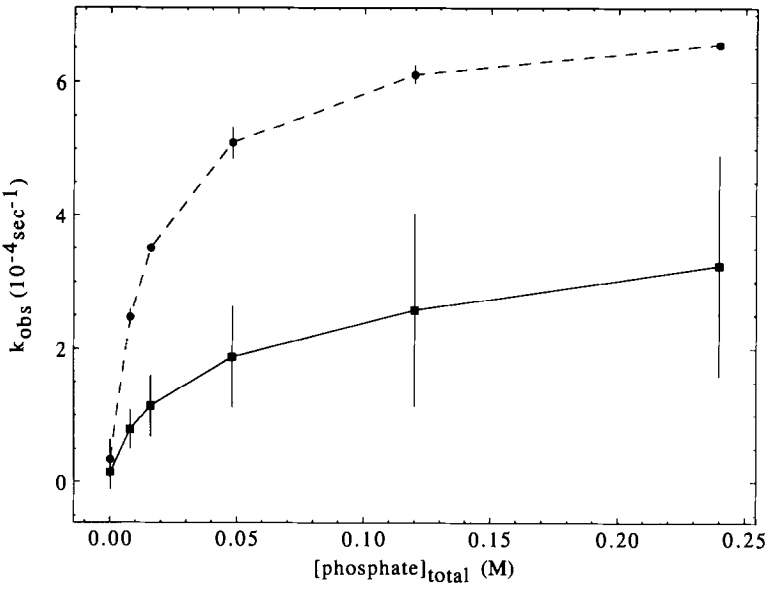

FIG. 2. The effects of phosphate buffer on the hydrolysis of **8** (■) and **9** (●). The lines are simple interpolations. The error bars represent 95% confidence limits, calculated from the SD of two or more measurements. T = 45°C, I = 1.0 M, pH 7.20.

(for instance, the twofold rate preference for the *para* isomer in the corresponding phosphonate diesters **8** and **9**).

In our previous study (*5*), phosphate buffer also reached kinetic saturation; bifunctional buffers have been shown to give saturation kinetics in other systems (*19*). The saturation can result from binding of the bifunctional buffer to the substrate or from a change in rate determining step. Our kinetic saturations with phosphate buffer were analyzed in terms of V_{max} and K_d by the usual double reciprocal plot. Linear least-squares fitting of the double reciprocal plots gave correlation coefficients greater than 0.99. The kinetic results are summarized in Table 1.

One might hope that the intramolecular catalysis in **4** would lead to a rate larger than that of the external catalysis of **6** even at kinetic saturation, but that is not the case. The V_{max} for *para* acid **6** is 3.4×10^{-4} s^{-1}, which is 80% greater than the rate constant for *ortho* acid **4**. This is not because a phosphate is a better catalyst than a phosphonate. We measured the rates of hydrolysis with methylphosphonate buffer. The *para* acid **3** hydrolyzes more quickly with added methylphosphonate, than with phosphate, while the *ortho* acid **2** is not affected by buffer over the concentration range studied, just as with phosphate buffer. The results are summarized in Fig. 3. Thus the faster maximum rate of *para* acid **6** relative to *ortho* acid **4** is probably caused by different steric/electronic effects, reflected also in the fact that the *para* diester **9** hydrolyzes about two times faster than *ortho* diester **8** (both with no added phosphate buffer).

TABLE 1

Calculated Maximum Rate Constants[a] with Phosphate Buffer

Substrate	k (no phosphate)	V_{max}	V_{max}/k (no phosphate)
4	1.8 ± 0.2	1.9 ± 0.2	1.1
5	~0.1[b]	1.3 ± 0.1	13
6	0.21 ± 0.04	3.4 ± 0.2	22
7	0.0042 ± 0.0029	0.01 ± 0.0003[c]	2.3
8	0.15 ± 0.11	3.0 ± 1	20
9	~0.3[d]	6.7 ± 0.2	16

[a] All rate constants in units 10^{-4} s^{-1}.
[b] Only one run.
[c] Rate constant at $[phosphate]_{total}$ = 1 M.
[d] Average of two runs with unusually large variation.

We suggested in our earlier paper that the saturation plateau we saw there occurs as the rate determining step changes from breakdown to formation of the tetrahedral intermediate (5). Considering the fact that methylphosphonate buffer produces a higher maximum rate than phosphate, we now propose that the plateau is instead due to saturation of binding of the substrate by the buffer. If the rate determining step were changing, one would expect the same plateau rate, corresponding to the new rate determining step, regardless of the type of buffer.

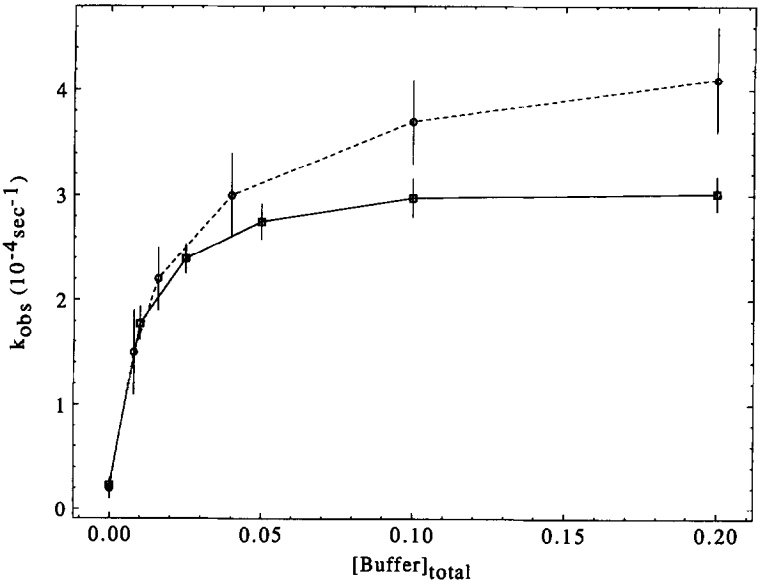

FIG. 3. The effects of methylphosphonate (○) and phosphate buffer (□) on the rate of hydrolysis of **6**. The lines are simple interpolations. The error bars represent 95% confidence limits, calculated from the SD of two or more measurements. T = 45°C, I = 1.0 M, pH 7.20.

The binding of the buffer to the substrate **6** could give a productive complex that hydrolyzes to products, or an unproductive complex that is a dead end, and still formally fit the kinetics. We favor productive binding, because a detailed kinetic analysis yields rate constants that seem more reasonable than those for the unproductive binding alternative.

pH-Rate Profiles

The rates of hydrolysis at different pH's have been measured for models **4** and **6** and are plotted as log (k_0) vs pH in Fig. 4. The rate constants shown are buffer independent rate constants k_0 (from the intercept of the pseudo-first-order rate constant vs buffer concentration, as described under Materials and Methods).

An unexpected feature of the pH-rate profiles is that the slopes are not unity over any part of the range studied. Normally the slope would be expected to be one for a hydrolysis reaction, such as amide hydrolysis, that has a first-order dependence on hydroxide. A slope less than one could occur at inflection points caused if a substrate group or a catalytic group, such as the phosphonate, titrates to a less reactive species. Phenylphosphonic acid has pK_{a1} of 1.83 and pK_{a2} 7.07 (*20*). The pK_a's of acids that ionize to anions are often lowered when the acid is near a cation (*4*). If the pK_{a2} of the phosphonic acid group in compound **4** were lowered to around 5.6, its titration could explain the flattened slope in the lower pH region. The curve would remain flattened if the amide proton titrated around pH 8.7. When chelated to cobalt, amide protons have pK_a's of 7 to 11.2 (*21, 22*).

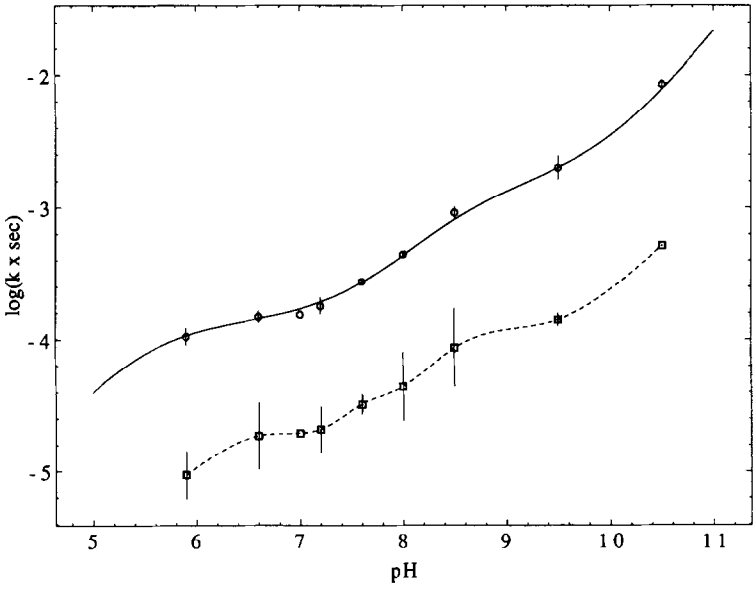

FIG. 4. pH-rate profiles for the hydrolysis of **4** (○) and **6** (□). Buffer uncatalyzed rate constants are used, as described in the text. The solid line is calculated using Eq. [2] and the values of the rate constants in Table 2. The dotted line is a computer-generated interpolation. The error bars represent 95% confidence limits, calculated from the SD of two or more measurements. T = 45°C, I = 1.0 M.

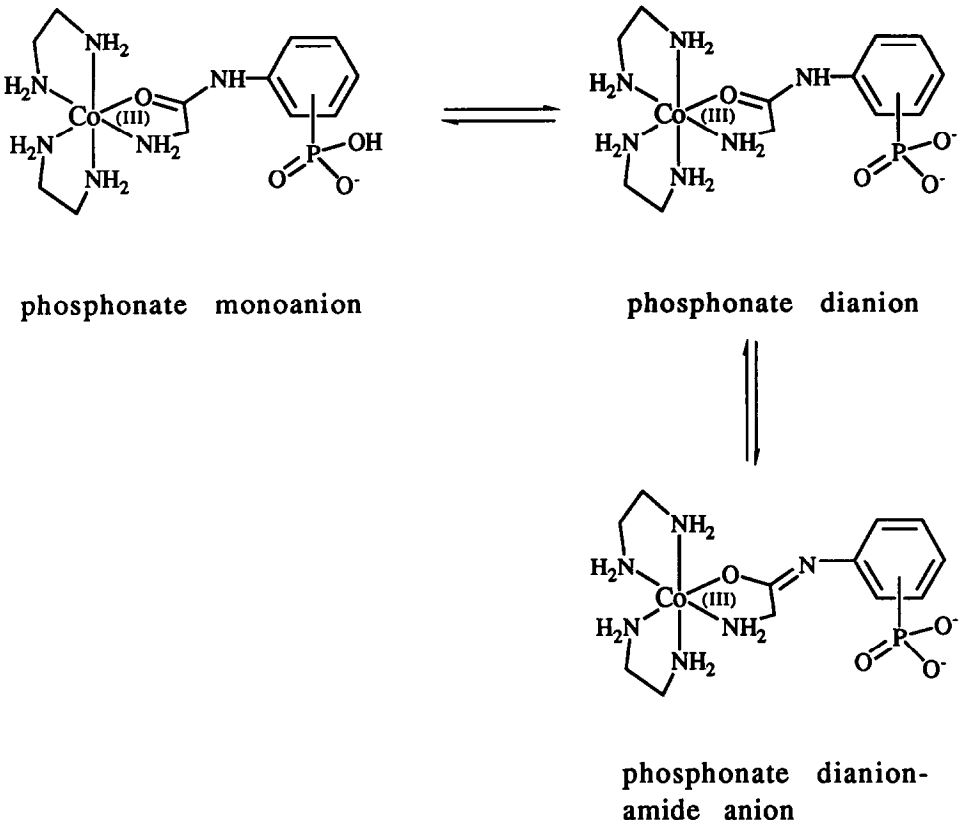

FIG. 5. The different protonation states of the complexes. The first pK_a is 5–6, and the second pK_a is 8–9.

The flattened pH-rate profiles can be explained by recognizing that in the pH region we are exploring the compounds can exist in three different protonation states (phosphonate monoanion, phosphonate dianion, and phosphonate dianion amide anion) each with a different hydrolysis rate (Fig. 5). The solid line was calculated using the following equations and using values for the rate constants listed in Table 2:

$$\text{rate} = k_3[SH_2] + k_4[SH] + k_5[S] = k_{obs}[\text{complex}]_{total} \quad [1]$$

$$k_{obs} = \{k_3K_w^2[OH^-] + K_1K_wk_4[OH^-]^2 + k_5K_1K_2[OH^-]^3\}/\{K_w^2 + K_1K_w[OH^-] + K_1K_2[OH^-]^2\}, \quad [2]$$

where $K_w = 1 \times 10^{-14}$.

These values were chosen by inspection and do not represent a unique solution. They do illustrate that a reasonable scheme can explain the flattening of the rate profiles.

The *ortho* compound **4** could hydrolyze more quickly than the *para* isomer **6** if it had a greater concentration of a more reactive form at the same pH. For example,

TABLE 2

Rate and Equilibrium Constants Used to Calculate the pH-Rate Profile for the Hydrolysis of **4**

Constant	Value S^{-1}
k_3	55000 M^{-1}
k_4	400 M^{-1}
k_5	20 M^{-1}
pK_1	5.4
pK_2	8.6

the pK_a of the amide proton might be raised by hydrogen bonding to the *ortho*-phosphonic acid anion. However, the pK_a of the amide proton in **4** is apparently not higher than that in **6**; the fact that the curves of Fig. 4 are parallel shows that the titratable groups have the same pK_a's in **4** and **6**. Thus it seems most likely that the different hydrolysis rates of the *ortho* and *para* isomers are due to intramolecular catalysis in the *ortho* compound.

The Rate Increase Attributable to Having an Anilide Leaving Group

The hydrolysis of the cyclohexyl amide **7** in the presence of various buffers was studied by HPLC. The results are summarized in Table 3. Cyclohexyl model **7** is 35 times slower than the *ortho* diester **8**, 430 times slower than *ortho* acid **4**, and 50 times slower than *para* acid **6**. Thus the models with an aniline leaving group hydrolyze one to two orders of magnitude faster than the model with a secondary amine leaving group.

Stereoelectronic Orientation in Phosphonic Acids

To be optimally effective a catalytic group must not only be near the reactive center, but must also have the correct stereoelectronic orientation. With carbox-

TABLE 3

Rate Constants for the Hydrolysis of **7** with Various Buffers[a]

Buffer	k_{obs} (10^{-7} s^{-1})
0.125 M Hepes	6.9 ± 1.4
0.175 M Hepes	6.8[b]
0.250 M Hepes	9.1 ± 6.0
0.70 M Phosphate	9.6 ± 2.5
1.0 M Phosphate	10.2 ± 1.1

[a] All buffers pH 7.20.
[b] Only one measurement.

ylate ions, Gandour postulates (*10*) that the *syn* lone pairs are much more basic than the *anti* lone pairs, and therefore that the *syn* lone pairs are catalytically more effective. In our previous models **1–3** an internal proton abstraction would require use of the less basic *anti* lone pairs, forming an *anti* conformation of the carboxyl group. The *syn* conformer of formic acid is calculated to be 4.5 kcal/mol more stable than the *anti* conformer.

We wondered if certain lone pairs in phosphonate anions might be more basic than others due to a stereoelectronic effect. Calculations of the conformational energy space for phosphonic acid, $HPO(OH)_2$, are available (*23*). There is still a preference for the acidic protons to be *syn* to the phosphoryl oxygen O, analogous to the proton being *syn* to the carbonyl in formic acid, but the preference is diminished. In phosphonic acid, a conformer exists with the hydrogens *anti* (179° from *syn*) to the phosphoryl oxygen, and it is calculated to be only 0.13 kcal/mol higher in energy than the *syn* ground state. From these calculations, the stereoelectronic effect on lone pair basicity in phosphonate anions is much smaller than in carboxylate ions. This less strict steric requirement in a phosphonic acid, in addition to a higher pK_a, makes the phosphonate group a better internal catalyst than a carboxylate ion in our compounds.

CONCLUSIONS

A phosphonate group is an effective internal catalyst for hydrolysis of an amide chelated to Co(III) and accounts for at least a ninefold additional rate acceleration in models where a carboxylate was ineffective. In the model **4** with a correctly positioned phosphonic acid, external bifunctional buffer does not affect the rate of hydrolysis. However, bifunctional buffers do affect the rate in other models, probably through an association mechanism. The pH-rate profiles show that the *ortho* acid **2** and the *para* acid **3** have the same pK_a's for the phosphonic acid and the amide proton. Similar pK_a's indicate that the rate increase in the *ortho* acid **2** is not because an intramolecular hydrogen bond between the amide proton and the phosphonate anion affects the pK_a of the amide proton.

The better catalytic ability of the phosphonate anion over a carboxylate can be attributed to two factors. First, a phosphonic acid has a relaxed stereoelectronic requirement; the orientation of its proton is not as strictly fixed as it is in formic acid. Second, the kinetic pK_{a2} of the phosphonic acids in the models is about 5.6, which is much higher than the pK_a of less than 2 for the carboxylic acids in previous models and close to the pK_a of the catalytic carboxylic acid of Glu-270 in CPA (pK_a 6.1). Other models that use a normal carboxylic acid to mimic a carboxylate in an enzymatic hydrophobic environment might also benefit if a phosphonic acid were used instead.

ACKNOWLEDGMENTS

Partial support of this work by the Office of Naval Research and an NSF Predoctoral Fellowship to J.L. are gratefully acknowledged.

REFERENCES

1. NEURATH, H. (1960) *in* The Enzymes (Boyer, P. D., and Myrback, K., Eds.), p. 11, Academic Press, New York. VALLEE, B. L., GALDES, A., AULD, D. S., AND RIORDAN, J. F. (1983) *in* Metal Ions in Biology (Spiro, T. G., Ed.), Wiley, New York. KAISER, E. T., AND KAISER, B. L. (1972) *Acc. Chem. Res.* **5,** 219.
2. CHRISTIANSON, D. W., AND LIPSCOMB, W. N. (1989) *Acc. Chem. Res.* **22,** 62–69.
3. MONZINGO, A. F., AND MATTHEWS, B. M. (1984) *Biochemistry* **23,** 5724–5730. HANGAUER, D. G., MONZINGO, A. F., AND MATTHEWS, B. M. (1984) *Biochemistry* **23,** 5730.
4. GROVES, J. T., AND CHAMBERS, R. R. (1984) *J. Amer. Chem. Soc.* **106,** 630.
5. SCHEPARTZ, A., AND BRESLOW, R. (1987) *J. Amer. Chem. Soc.* **109,** 1814–1826.
6. BRESLOW, R., AND SCHEPARTZ, A. (1987) *Chem. Lett.,* 1–4.
7. BRESLOW, R., AND WERNICK, D. L. (1976) *Proc. Natl. Acad. Sci. USA* **74,** 1303.
8. BUCKINGHAM, D. A., DAVIS, C. E., FOSTER, D. M., AND SARGESON, A. M. (1970) *J. Amer. Chem. Soc.* **92,** 5571. BUCKINGHAM, D. A., FOSTER, D. M., AND SARGESON, A. M. (1970) *J. Amer. Chem. Soc.* **92,** 6151. BUCKINGHAM, D. A., KEENE, F. R., AND SARGESON, A. M. (1974) *J. Amer. Chem. Soc.* **96,** 4981.
9. GARDELL, S. J., CRAIK, C. S., HILVERT, D., URDEA, M. S., AND RUTTER, W. J. (1985) *Nature (London)* **317,** 551.
10. GANDOUR, R. D. (1981) *Bioorg. Chem.* **10,** 169.
11. SPRATT, T. E., SUGIMOTO, T., AND KAISER, E. T. (1983) *J. Amer. Chem. Soc.* **105,** 3579.
12. GORENSTEIN, D. G. (1987) *Chem. Rev.* **87,** 1047–1077.
13. BULOT, J., ABOUJAOUDE, E., COLLIGNON, N., AND SAVIGNAC, P. (1984) *Phosphorous Sulfur* **21,** 197.
14. COLLINS, D. J., DRYGALA, P. E., AND SWAN, J. M. (1982) *Tetrahedron Lett.* **23,** 1117.
15. NAYLOR, R. A., AND WILLIAMS, A. (1976) *J. Chem. Soc. Perkin 2* **15,** 1908.
16. JACKSON, W. G., BEGBIE, C. M., DASH, A. C., AND HARRIS, G. M. (1982) *in* Inorganic Syntheses (Fackler, J. P., Ed.), p. 119, Wiley, New York.
17. HARRISON, R. G., AND NOLAN, K. B. (1982) *J. Chem. Educ.* **59,** 1054.
18. SWAIN, C. G., SWAIN, M. S., AND BERG, L. F. (1980) *J. Chem. Inf. Comput. Sci.* **20,** 47.
19. LEE, Y.-N., AND SCHMIR, G. L. (1979) *J. Amer. Chem. Soc.* **101,** 3026–3035. COX, M. M., AND JENCKS, W. P. (1981) *J. Amer. Chem. Soc.* **103,** 580–587.
20. JAFFÉ, H., FREEDMAN, L., AND DOAK, G. (1953) *J. Amer. Chem. Soc.* **75,** 2209.
21. SCHEPARTZ, A. (1986) Ph.D. thesis, Columbia University, New York, p. 60.
22. BUCKINGHAM, D. A., DAVIS, C. E., FOSTER, D. M., AND SARGESON, A. M. (1970) *J. Amer. Chem. Soc.* **92,** 5571.
23. EWIG, S. S., AND VAN WAZER, J. R. (1985) *J. Amer. Chem. Soc.* **107,** 1965.